IJEMD-M, 4 (1) (2026) https://doi.org/10.54938/ijemdm.2026.04.1.701

IJEMD

International Journal of Emerging Multidisciplinaries: Mathematics

Research Paper

Journal Homepage: www.ojs.ijemd.com

ISSN (print): 2790-1998

Dielectric Properties of PVDF and G4/T10/PVDF Composites Using the Debye Relaxation Model

J. A. Ukwenya [1]*, J. A. Owolabi[2], M. Y. Onimisi [2], T. J. Ikyumbur [3], A. J. Okemsinachi [4] and O. E. Jayeola [5]

1. Department of Physics, Federal College of Education, Yauri, Kebbi State, Nigeria.
2. Department of Physics, Nigerian Defence Academy (NDA), Kaduna State, Nigeria.
3. Department of Physics, Benue State University, Makurdi, Benue State, Nigeria.
4. Department of Physics, Greenfield University, Kaduna State, Nigeria.
5. Department of Physics, Federal College of Forestry Mechanisation, Kaduna State, Nigeria.

Abstract

The demand for advanced radar absorbing materials (RAMs) in stealth technology and electromagnetic interference (EMI) shielding necessitates the development of lightweight, highly efficient polymer composites. This work investigates the frequency and temperature dependent dielectric properties of polyvinylidene fluoride (PVDF) and (G4/T10/PVDF). Utilizing the Debye relaxation model, a computational framework was developed using Maple 18 to simulate the dielectric constant and loss factor across the microwave frequency range of 0.50 to 21.0 GHz and temperatures from 20 °C to 100 °C. Results indicate that the dielectric constant of both materials exhibits typical dispersion behavior, decreasing with increasing frequency. However, the G4/T10/PVDF composite demonstrates significantly enhanced dielectric properties, with a dielectric constant of 42.0 compared to 20.5 for PVDF at 0.5 GHz. This behaviour exhibited by G4/T10/PVDF showed that even as the frequency and temperature become very high G4/T10/PVDF does not produce too much heat which may be the reason for reducing object detectability and electromagnetic interference (EMI) by radar.

Keywords: Graphene; Titania; Debye relaxation model; Dielectric properties; Microwave absorption; Radar absorbing materials; Polyvinylidene fluoride (PVDF).

Email Address : amuchijessica@gmail.com

1. Introduction

The increased interest in radar absorber materials (RAMs) has been driven by the rapid advancement of radar technology in communication systems and microwave frequency which has driven the need for advanced RAMs. These materials are designed to attenuate electromagnetic waves (EMW) by converting it energy to thermal energy, thereby reducing electromagnetic interference (EMI) and objects detectability by radar [1]. As modern electronic systems demand highly sensitive and wider frequency, particularly for 5G and 6G technologies, the development of lightweight, flexible, and highly effective RAMs has become a focal point in materials science [2, 3].

Polyvinylidene fluoride (PVDF) is a semi-crystalline fluoropolymer widely used for its excellent chemical resistance, thermal stability, mechanical flexibility, and inherent piezoelectric properties [4]. However, the practical application of pure PVDF as a RAM is limited by its relatively low dielectric constant and intrinsic electrical conductivity, which restrict its electromagnetic wave absorption [5]. These limitations can be overcome through incorporation of conductive and dielectric nanofillers into the PVDF dielectric matrix emerging as a highly effective technique. PVDF is called a dielectric matrix because it is an insulating material that stores electrical energy, support dipole polarization and holds graphene and titania fillers together. Currently research of hybrid fillers has highlighted its efficiency as in graphene combined with metal oxides and in generating effective synergy that increase impedance matching and attenuation capabilities [6, 7].

Carbon-based RAMs, especially graphene is highly electrically conductive and has large surface area which makes them suitable for enhancing dielectric loss i.e. the actual physical energy dissipated as heat through conduction loss and polarization mechanisms [8]. The dielectric ceramic like titania when incorporated with graphene and PVDF forms interfaces between them which is called interfacial polarization to improve electromagnetic wave absorption [9]. In this work, the G4/T10/PVDF composite-comprising a PVDF matrix reinforced exhibit a promising alternative for next-generation RAMs [10].

Despite the excellent quality of such composites, a comprehensive understanding of their dielectric relaxation behavior across wide microwave frequency region and varying thermal conditions remains limited. Experimental characterization of these parameters is often complex, time-consuming, and costly [11]. Therefore, this study provides an adaptative computational framework based on the Debye relaxation model and its related formulations to systematically investigate and compare the dielectric properties (dielectric constant and loss factor) of PVDF and G4/T10/PVDF. By simulating the material response from 0.50 GHz to 21.0 GHz and 20 °C to 100 °C, this research aims to showcase the underlying polarization mechanisms and identify the optimal performance for advanced microwave absorption applications, addressing the gap in theoretical validation for hybrid carbon-ceramic polymer composites [12, 13].

2. Theoretical Framework

The dielectric material is fundamentally governed by its complex permittivity (ε^*) through the interaction of electromagnetic waves, which describes the material's ability to store and dissipate electrical energy when subjected to an electric field is expressed in equation (1):

$$\varepsilon^* = \varepsilon' - \mathrm{j}\varepsilon'' \quad (1)$$

where the complex permittivity is ε^*which is a combination of both the real part (ε') known as the dielectric constant, representing energy storage, and the imaginary part (ε'') known as the dielectric loss factor, representing energy dissipation [14].

2.1 The Cole-Cole Relaxation Model

The presence of filler-matrix interfaces in composite materials such as G4/T10/PVDF, varying with applied electric fields and structural heterogeneity which result in a relaxation times distribution rather than a single relaxation time. The Cole-Cole model modifies the Debye equation by introducing a broadening parameter α ($0 \leq \alpha \leq 1$) in other to account for symmetric broadening of the relaxation spectrum:

$$\varepsilon^*(\omega) = \varepsilon_\infty + \frac{\varepsilon_s - \varepsilon_\infty}{1+(j\omega\tau)^{1-\alpha}} \quad (2)$$

Equation (5) reduces to the ideal Debye relaxation model only when $\alpha = 0$. If $\alpha > 0$ for G4/T10/PVDF composite is utilized to capture the non-ideal and distributed relaxation dynamics arising from interfacial (Maxwell-Wagner-Sillars) polarization [16].

Recall from equation (1) that $\varepsilon^* = \varepsilon' - \mathrm{j}\varepsilon''$

$$\varepsilon^* = \varepsilon_\infty + \frac{(\varepsilon_s - \varepsilon_\infty)\left[1+(\omega\tau)^{1-\alpha}\sin\left(\alpha\pi/2\right)\right]}{1+2(\omega\tau)^{1-\alpha}\sin\left(\alpha\pi/2\right)+(\omega\tau)^{2(1-\alpha)}} - \mathrm{j}\,\frac{(\varepsilon_s - \varepsilon_\infty)(\omega\tau)^{1-\alpha}\cos\left(\alpha\pi/2\right)}{1+2(\omega\tau)^{1-\alpha}\sin\left(\alpha\pi/2\right)+(\omega\tau)^{2(1-\alpha)}} \quad (3)$$

The real and imaginary components of the Cole-Cole relaxation model is given by:

$$\varepsilon'(\omega) = \varepsilon_\infty + \frac{(\varepsilon_s - \varepsilon_\infty)\left[1+(\omega\tau)^{1-\alpha}\sin\left(\alpha\pi/2\right)\right]}{1+2(\omega\tau)^{1-\alpha}\sin\left(\alpha\pi/2\right)+(\omega\tau)^{2(1-\alpha)}} \quad (4)$$

and the imaginary component is:

$$\varepsilon''(\omega) = \frac{(\varepsilon_s - \varepsilon_\infty)(\omega\tau)^{1-\alpha}\cos\left(\alpha\pi/2\right)}{1+2(\omega\tau)^{1-\alpha}\sin\left(\alpha\pi/2\right)+(\omega\tau)^{2(1-\alpha)}} \quad (5)$$

2.2 The Debye Relaxation Model

The Debye relaxation model is used to described the dielectric relaxation behaviour of a material, and it assumes that all dipoles in the material relax independently with a single relaxation time. The complex permittivity (ε^*) of a dielectric material is given by:

$$\varepsilon^* = \varepsilon_\infty + \frac{(\varepsilon_s - \varepsilon_\infty)}{(1 + j\omega\tau)} \quad (6)$$

where the static permittivity at low frequency is ε_∞, the high-frequency permittivity is ε_s, angular frequency ω, and τ is the relaxation time which separate both the real and imaginary parts:

$$\varepsilon' = \varepsilon_\infty + \frac{(\varepsilon_s - \varepsilon_\infty)}{(1 + \omega^2\tau^2)} \quad (7)$$

$$\varepsilon'' = \frac{(\varepsilon_s - \varepsilon_\infty)\omega\tau}{(1 + \omega^2\tau^2)} \quad (8)$$

While the Debye model accurately describes the dipolar relaxations in PVDF, it often explained the behavior of heterogeneous nanocomposites [15]. The Debye model parameters of PVDF and G4/T10/PVDF composites were written in the interactive environment of maple-18 [13].

3. Methodology

In this part under the methodology, the physical parameters required for the simulating static permittivity, high-frequency permittivity, electrical conductivity, and relaxation time, were adapted from literature [18–20]. This radar absorber materials (RAMs) was chosen because the are applicable for communication devices and defense system in both communication and stealth technologies.

3.2 Computational Method

The computational framework was developed and executed using Maple-18, a symbolic and numerical computing environment. The simulation covered a microwave frequency range of 0.50 GHz to 21.0 GHz and a temperature range of 20 °C to 100 °C. An algorithm was designed to systematically calculate the dielectric parameters of PVDF and the Debye model was applied. For the G4/T10/PVDF composite was utilized to account for the distribution of relaxation times. The algorithm computed the real and imaginary parts of the complex permittivity, from which the loss tangent and attenuation constants were subsequently derived. The resulting data were visualized to analyze dielectric dispersion, loss mechanisms, and attenuation behavior under varying thermal and electromagnetic conditions.

Therefore, the dielectric response of PVDF and G4/T10/PVDF in the gigahertz frequency and temperature ranges were fitted with theoretical models based on the Debye model were compared to evaluate their suitability in describing dielectric behaviour. The comparison provides insight into the influence of distributed relaxation processes on the dielectric response of PVDF and G4/T10/PVDF shows that both models can be utilized for high-frequency dielectric characterization. Results generated from maple-18 was copy and pasted into origin to plot graphs for dielectric constant and loss factor. This result was obtained using equations (7) and (8) shown in the Tables below:

Table 1: Dielectric constant and loss factor of PVDF at different temperatures

	20°C		40°C		60°C		80°C	
F (GHz)	ε'	ε''	ε'	ε''	ε'	ε''	ε'	ε''
0.5	20.49	0.37	20.5	0.19	20.5	0.12	20.5	0.09
0.75	20.39	1.49	20.47	0.75	20.49	0.5	20.49	0.37
1.5	20.17	2.58	20.41	1.31	20.46	0.87	20.48	0.66
2.25	19.84	3.63	20.33	1.86	20.42	1.24	20.46	0.94
3	19.4	4.61	20.21	2.4	20.37	1.61	20.43	1.21
3.75	18.88	5.52	20.07	2.94	20.31	1.98	20.39	1.49
4.5	18.29	6.36	19.9	3.46	20.23	2.34	20.34	1.77
5.25	17.64	7.1	19.7	3.96	20.14	2.7	20.29	2.04
6	16.96	7.75	19.48	4.45	20.03	3.05	20.24	2.31
6.75	16.24	8.32	19.24	4.92	19.92	3.4	20.17	2.58
7.5	15.51	8.79	18.98	5.38	19.79	3.74	20.1	2.85
8.25	14.78	9.19	18.69	5.81	19.66	4.07	20.01	3.11
9	14.06	9.51	18.39	6.22	19.51	4.4	19.93	3.37
9.75	13.35	9.77	18.08	6.61	19.35	4.72	19.84	3.63
10.5	12.67	9.96	17.76	6.98	19.18	5.03	19.74	3.88
11.25	12.01	10.1	17.42	7.33	19.01	5.33	19.63	4.13
12	11.37	10.19	17.07	7.65	18.82	5.62	19.52	4.37
12.75	10.77	10.24	16.72	7.95	18.63	5.9	19.4	4.61
13.5	10.19	10.25	16.36	8.23	18.43	6.18	19.28	4.85
14.25	9.65	10.23	16	8.48	18.22	6.44	19.15	5.08
15	9.13	10.19	15.64	8.72	18.01	6.7	19.02	5.3
15.75	8.65	10.12	15.27	8.94	17.79	6.94	18.88	5.52
16.5	8.2	10.04	14.91	9.13	17.57	7.17	18.74	5.74
17.25	7.77	9.94	14.54	9.31	17.34	7.4	18.6	5.95
18	7.37	9.84	14.18	9.47	17.11	7.61	18.45	6.16
18.75	6.99	9.72	13.82	9.61	16.88	7.82	18.29	6.36
19.5	6.64	9.59	13.47	9.73	16.64	8.01	18.13	6.55
20.25	6.31	9.46	13.12	9.84	16.4	8.2	17.97	6.74
21	6	9.33	12.78	9.93	16.16	8.37	17.81	6.92

Table 2: Dielectric constant and loss factor of PVDF at temperatures 100 °C

F (GHz)	ε'	ε''
0.5	20.5	0.09
0.75	20.49	0.37
1.5	20.48	0.66
2.25	20.46	0.94
3	20.43	1.21
3.75	20.39	1.49
4.5	20.35	1.77
5.25	20.3	2.04
6	20.24	2.31
6.75	20.17	2.58
7.5	20.1	2.85
8.25	20.02	3.11
9	19.93	3.37
9.75	19.84	3.63
10.5	19.74	3.88
11.25	19.63	4.13
12	19.53	4.37
12.75	19.4	4.61
13.5	19.28	4.85
14.25	19.15	5.08
15	19.02	5.3
15.75	18.88	5.52
16.5	18.74	5.74
17.25	18.6	5.95
18	18.45	6.16
18.75	18.29	6.35
19.5	18.13	6.55
20.25	17.97	6.74
21	17.81	6.92

Table 3: Dielectric constant and loss factor of G4/T10/PVDF at different temperatures

	20°C		40°C		60°C		80°C	
F (GHz)	ε'	ε''	ε'	ε''	ε'	ε''	ε'	ε''
0.5	42.04	0.74	42.05	0.37	42.05	0.25	42.05	0.19
0.75	41.844	2.95	42	1.48	42.03	0.99	42.04	0.74
1.5	41.42	5.16	41.89	2.59	41.98	1.73	42.01	1.3
2.25	40.78	7.2	41.73	3.68	41.9	2.47	42	1.85
3	39.95	9.16	41.5	4.76	41.81	3.2	41.91	2.4
3.75	38.94	11	41.22	5.82	41.68	3.92	41.84	2.95
4.5	37.8	12.67	40.9	6.86	41.53	4.64	41.76	3.5
5.25	36.54	14.19	40.52	7.87	41.36	5.35	41.66	4.04
6	35.2	15.53	40.1	8.86	41.16	6.05	41.54	4.58
6.75	33.8	16.7	39.63	9.79	40.94	6.74	41.42	5.12
7.5	32.36	17.71	39.12	10.7	40.7	7.42	41.28	5.65
8.25	30.91	18.55	38.58	11.57	40.43	8.09	41.12	6.17
9	29.48	19.25	38	12.41	40.15	8.74	40.96	6.69
9.75	28.06	19.81	37.39	13.2	39.84	9.38	40.78	7.2
10.5	26.68	20.25	36.76	13.94	39.52	10	40.59	7.7
11.25	25.35	20.58	36.1	14.65	39.18	10.6	40.38	8.2
12	24.06	20.8	35.43	15.32	38.82	11.19	40.17	8.68
12.75	22.83	20.95	34.74	15.94	38.45	11.76	39.95	9.16
13.5	21.65	21.02	34.03	16.52	38.07	12.31	39.71	9.64
14.25	20.53	21.02	33.32	17.05	37.67	12.85	39.47	10.1
15	19.48	20.97	32.6	17.55	37.25	13.37	39.21	10.55
15.75	18.48	20.87	31.88	18.01	36.83	13.87	38.94	11
16.5	17.53	20.73	31.16	18.42	36.4	14.35	38.67	11.43
17.25	16.65	20.56	30.44	18.8	35.95	14.81	38.39	11.86
18	15.81	20.37	29.72	19.14	35.5	15.25	38.1	12.27
18.75	15.02	20.15	29.01	19.45	35.04	15.67	37.8	12.67
19.5	14.28	19.92	28.3	19.73	34.58	16.07	37.49	13.07
20.25	13.59	19.67	27.6	19.97	34.11	16.46	37.18	13.45
21	12.94	19.41	26.91	20.18	33.64	16.82	36.87	13.82

Table 4: Dielectric constant and loss factor of G4/T10/PVDF at temperatures 100 °C

F (GHz)	ε'	ε''
0.5	42.05	0.15
0.75	42.04	0.59
1.5	42.02	1.04
2.25	42	1.48
3	41.96	1.93
3.75	41.92	2.37
4.5	41.86	2.81
5.25	41.8	3.25
6	41.73	3.68
6.75	41.64	4.12
7.5	41.55	4.55
8.25	41.45	4.97
9	41.34	5.4
9.75	41.23	5.82
10.5	41.1	6.24
11.25	40.97	6.65
12	40.83	7.06
12.75	40.67	7.47
13.5	40.52	7.87
14.25	40.36	8.26
15	40.19	8.65
15.75	40.01	9.04
16.5	39.82	9.42
17.25	39.63	9.79
18	39.43	10.16
18.75	39.23	10.52
19.5	39.02	10.88
20.25	38.8	11.23
21	38.58	11.57

4. Discussion

4.1 Variation of Dielectric Constant with Frequency for PVDF

Figure 1 illustrates the frequency-dependent dielectric dispersion behavior of the material at different temperatures. At low frequencies (around 0.5 GHz), the dielectric constant exhibits a relatively high value (≈ 20.49), which gradually decreases as the frequency increases. This trend is characteristic of dielectric relaxation and is primarily attributed to the reduced ability of polarization mechanisms such as interfacial (Maxwell–Wagner), dipolar, and space-charge polarization to follow the rapidly oscillating electric field at higher frequencies. At low frequencies, these polarization processes have sufficient time to align with the applied field, resulting in enhanced charge accumulation and a higher dielectric constant.

As the frequency continues to increase, the dielectric constant approaches a nearly constant value, indicating the dominance of faster polarization mechanisms, particularly electronic polarization, which can respond even at microwave frequencies. The observed stabilization of the dielectric constant at high frequencies reflects the suppression of slower polarization processes and the intrinsic response of the material's electronic structure.

Temperature also plays a significant role in this dielectric behavior. At elevated temperatures, increased thermal energy enhances charge carrier mobility and facilitates dipolar orientation within the PVDF polymer matrix, contributing to higher dielectric values at lower frequencies. However, as frequency increases, the influence of temperature diminishes because thermal activation cannot compensate for the limited response time of slower polarization mechanisms. This combined frequency–temperature dependence highlights the suitability of PVDF-based materials for microwave applications, where controlled dielectric dispersion and stable high-frequency behavior are desirable.

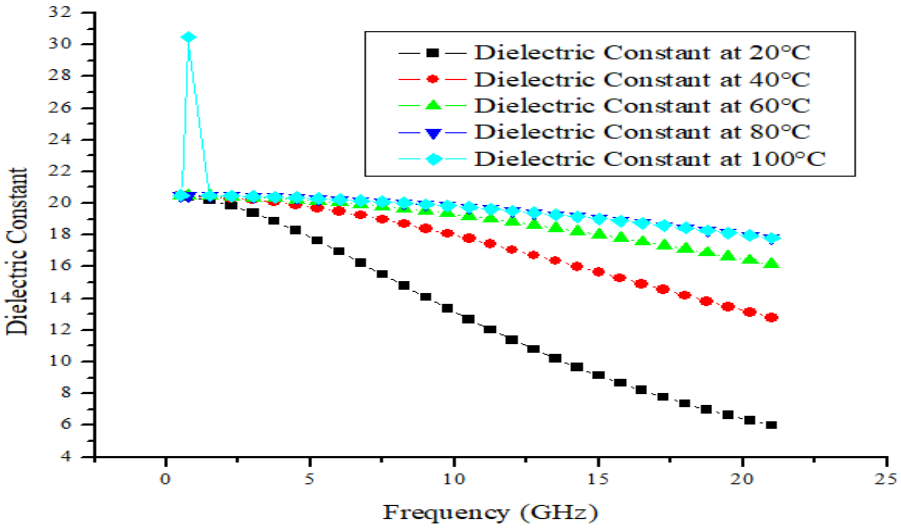

Figure 1: Variation of dielectric constant with frequency for PVDF over the temperature range of 20 –100 °C

4.2 Variation of Dielectric Constant with Frequency for G4/T10/PVDF

Figure 2 illustrates the frequency-dependent variation of the dielectric constant of G4/T10/PVDF over the temperature range of 20 °C to 100 °C. At all investigated temperatures, the dielectric constant exhibits a relatively high value (≈ 42.04) at low frequencies (around 0.5 GHz) and decreases progressively with increasing frequency, which is a typical dielectric dispersion behavior.

At lower frequencies, dipolar entities and mobile charge carriers within the G4/T10/PVDF composite are able to respond effectively to the applied alternating electric field, leading to enhanced polarization and a correspondingly high dielectric constant. As the frequency increases, the response time of these polarization mechanisms becomes insufficient to follow the rapidly oscillating field, resulting in reduced dipolar alignment and interfacial polarization. Consequently, the dielectric constant decreases with increasing frequency.

The observed dielectric response of G4/T10/PVDF can be attributed to the combined contributions of dipolar orientation and interfacial (Maxwell–Wagner–Sillars) polarization arising from the heterogeneous interfaces between PVDF, graphene, and titania. This behavior confirms the suitability of G4/T10/PVDF for microwave applications, where controlled dielectric dispersion and enhanced polarization mechanisms are desirable.

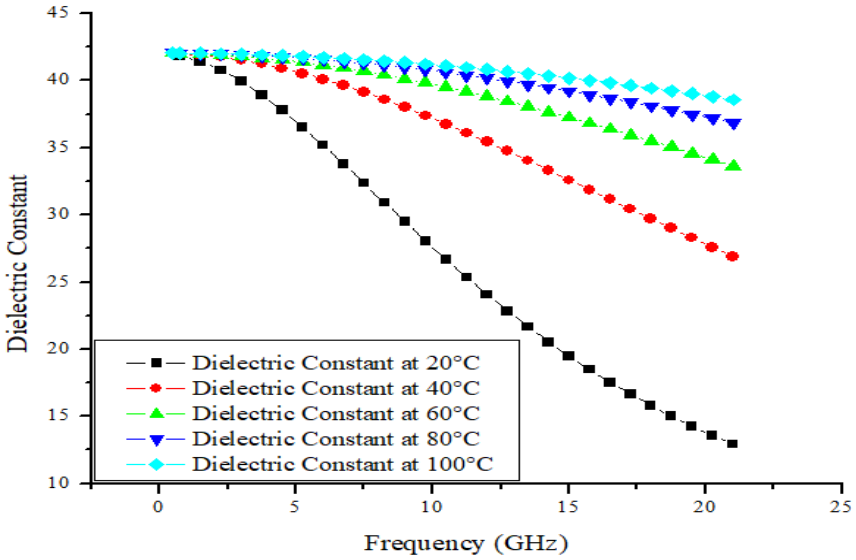

Figure 2: Variation of dielectric constant with frequency for G4/T10/PVDF over the temperature range of 20 –100 °C

4.3 Variation of Loss Factor with Frequency for PVDF

Figure 3 shows the frequency dependence of the dielectric loss factor (ε″) of PVDF at different temperatures. For all temperatures, the loss factor increases with increasing frequency, indicating enhanced dielectric losses at higher frequencies due to the growing phase lag between the applied alternating electric field and the polarization response.

Within the frequency range of 0.5–21.0 GHz, the loss factor reaches a maximum value of approximately 9.33 at 20 °C and gradually decreases as the temperature increases beyond 40 °C. This behavior is attributed to dielectric relaxation processes and variations in charge carrier mobility within the PVDF polymer matrix, which influence energy dissipation through conduction and dipolar relaxation mechanisms.

At higher frequencies, the separation between the loss factor curves becomes more pronounced, reflecting the increased sensitivity of dielectric loss mechanisms to thermal activation in this frequency region. As frequency increases, polarization processes struggle to follow the rapidly oscillating electric field, resulting in greater energy dissipation and a stronger temperature-dependent response.

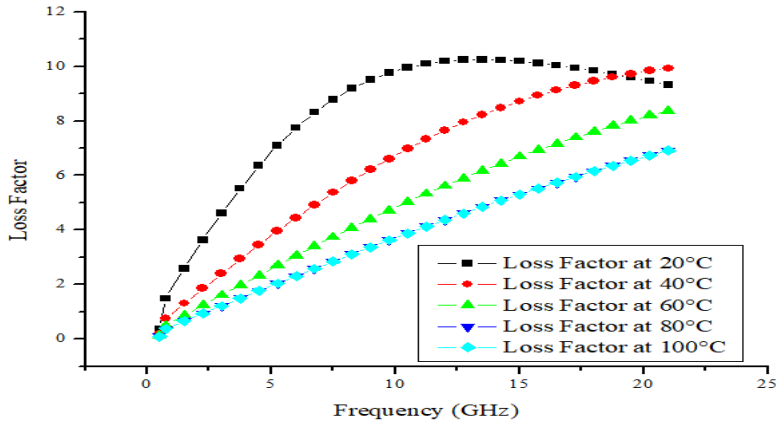

Figure 3: Variation of dielectric constant with frequency for PVDF over the temperature range of 20 –100 °C

4.4 Variation of Loss Factor with Frequency for G4/T10/PVDF

Figure 4 illustrates the frequency-dependent variation of the dielectric loss factor (ε″) for G4/T20/PVDF over the temperature range of 20–100 °C. For all temperatures, the loss factor increases steadily with increasing frequency, indicating that G4/T20/PVDF exhibits enhanced microwave energy dissipation at higher frequencies. At the maximum frequency, the loss factor reaches approximately 32.49 at the lowest temperature (20 °C) and gradually decreases as the temperature rises from 40 °C to 100 °C.

This trend suggests that at lower temperatures, polarization mechanisms particularly interfacial (Maxwell–Wagner) and dipolar polarization are more effective, resulting in higher dielectric losses. As temperature increases, thermal agitation disrupts the alignment of dipoles and reduces the efficiency of interfacial charge accumulation, leading to lower loss factor values.

Overall, the data demonstrate that G4/T20/PVDF offers superior attenuation capability at higher frequencies and lower operating temperatures, highlighting the synergistic effect of graphene oxide and titanium dioxide fillers in enhancing dielectric loss and microwave energy dissipation in polymer composites.

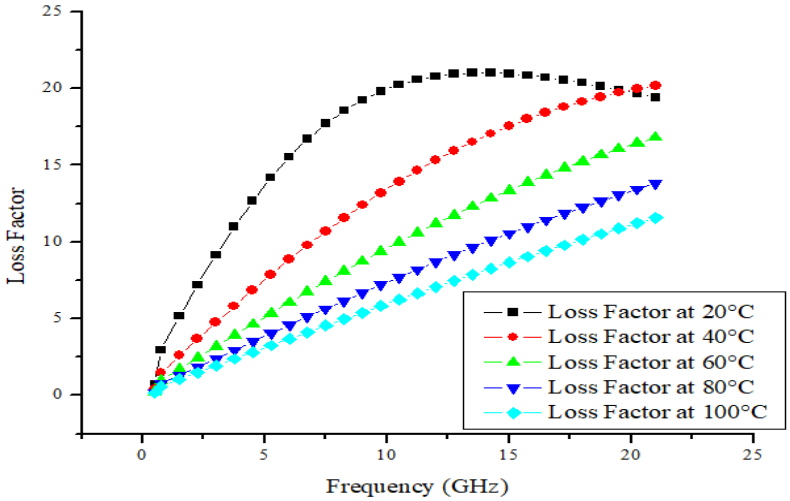

Figure 4: Variation of dielectric constant with frequency for G4/T10/PVDF over the temperature range of 20 –100 °C

5. Conclusion

The work successfully developed and executed a computational framework using Maple-18 to investigate the dielectric properties of pure PVDF and its composites has been computed using Debye relaxation model. The result from our computation showed that PVDF has a dielectric constant of 20.5 and loss factor of 0.19 while G4/T10/PVDF has higher dielectric constant of 42.05 and loss factor of 0.37 at low frequencies of 0.5GHz and temperatures of 40 °C. This higher dielectric constant at low frequencies and temperatures may be the reason why the composite of the radar absorbs more electromagnetic wave absorption. The value of the loss factor for material at those frequencies and temperatures as shown in Figure 4 simply mean G4/T10/PVDF does not generate too much heat when subjected to an applied electric field. It can be said that the loss factor decreases continuously after attaining its maximum value in Figure 4 above. This behaviour exhibited by G4/T10/PVDF showed that even as the frequency and temperature become very high G4/T10/PVDF does not produce too much heat which may be the reason for reducing object detectability and electromagnetic interference (EMI) by radar.

References

[1] Zhang, Y., Seul-Yi L., Soo-Jin P., & Junwei G. (2024). "Advanced Radar Absorbing Materials for Stealth Technology: A Review of Recent Progress." Progress in Materials Science, 12(3), 45-62.

[2] Li, X., & Wang, J. (2025). "Electromagnetic Interference Shielding in 6G Communications: Challenges and Material Solutions." IEEE Transactions on Electromagnetic Compatibility, 67(1), 112-125.

[3] Wen, Z., Tan, Y., Ji, S., Zhao, Y., & Li, T. (2013). Flexible and high-performance Piezocomposite generators based on BaTiO nanoparticles and PVDF. Journal of Applied Physics, 114(11), 114301.

[4] Chen, X., Han, X., & Shen, Q. D. (2017). PVDF-Based Ferroelectric Polymers in Modern Flexible Electronics, Adv Electron Mater 3(5).

[5] Dang, Z. M., Yuan, J. K., Yao, S. H., & Liao, R. J. (2013). Flexible nanodielectric materials With high permittivity for power energy storage. *Advanced Materials*, 25(44), 6334–6365.

[6] Seong H. K., Seul Y. L., Yali Z., Soo J. P., & Junwei G. (2023). "Carbon-Based Radar Absorbing Materials Toward Stealth Technologies." Advanced Science, 10(32), 2301456.

[7] Zhao, L., & Zhao, T. (2019). Research on Design and Application of Absorbing Material Based on Electromagnetic Compatibility of Handheld Device, IOP Conf. Ser.: Mater. Sci. Eng. 677-022016.

[8] Shorstkii, I., & Sosnin, M. (2024). "Graphene Oxide Derivatives for Enhanced Microwave Absorption." Carbon, 215, 118-130.

[9] Peng, Z.H., Peng, J.C., Peng, Y.F. & Wang, J.Y. (2008). Complex Conductivity and Permittivity of Single Wall Car bon Nanotubes/Polymer Composite at Microwave Frequencies: A Theoretical Estimation. Chinese Science Bulletin, 53 3497-3504.

[10] Ishaq, S., Kanwal, F., Atiq, S., Moussa, M., Azhar, U., & Losic, D. (2020). "Dielectric Properties of Graphene/Titania/Polyvinylidene Fluoride Nanocomposites." Journal of Composite Materials, 58(4), 567-580.

[11] Micheli, D., Roberto, P., Vricella, A., & Mario, M. (2014). Synthesis and electromagnetic

characterization of frequency selective radar absorbing materials using carbon nano-powders. Carbon. 77:756-74.

[12] Qin, M., & Brosseau, C. (2024). "Dielectric Loss Mechanisms in Electromagnetic Wave Absorbing Materials." Advanced Science, 11(5), 2305678.

[13] Chen, C., Pan, L., Jiang, S., Yin, S., Li, X., Zhang, J., & Yang, J. (2018). Electrical conductivity, dielectric and microwave absorption properties of graphene nanosheets/magnesia composites. Journal of the European Ceramic Society, 38(4), 1639- 1646.

[14] Kremer, F., & Schönhals, A. (2003). Broadband Dielectric Spectroscopy. Berlin: Springer.

[15] Antara, B., Preethi, K. R. S. M., & Varma, K. B. R. (2011). Dielectric Relaxation Behaviour of SR2SbMnO6 Ceramics fanricated from nanocrystalline powders prepared by molten salt synthesis. Bull. Matter Science 44(1).

[16] Ikyumbur, T. J., Asagha, E. N., Hemba1, E. C., & Bash, J. A. (2017). Dielectric Properties of 1 ethyl-3-methyl-imidazolium Tetrafluoroborate (EMIM-BF4) Using Cole-Cole Relaxation Model. Physical Science International Journal 13(3): 1-6; Article

[17] Huang, X., Leng, T., Georgiou, T., Abraham, J., Nair, R. R., Novoselov, K. S., & Hu, R. (2018). Graphene Oxide Dielectric Permittivity at GHz and Its Applications for Wireless Humidity Sensing, Science. Reports, 8:43.

[18] Rubrice, K., Castel, X., Himdi, M., & Parneix, P. (2016). Dielectric Characteristics and Microwave Absorption of Graphene Composite Materials, *Mater.*, 9825.

[19] Saira, I., Farah, K., Shahid, A., Mahmoud, M., Umar, A., & Dusan, L. (2020). Dielectric Properties of Graphene/Titania/Polyvinylidene Fluoride (G/TiO2/PVDF) Nanocomposites. Materials,13:205.

[20] Rani, P., Deshmukh, K., Kadlec, J., Krishna, K. T. V., & Khadheer, P. S. K. (2023). Dielectric properties of graphene/nano-Fe2O3 filled poly (vinyl alcohol)/Chitosan blends. Materials Science and Engineering: B, 282:115688.

[21] Huang, X., Leng, T., Georgiou, T., Abraham, J., Nair, R. R., Novoselov, K. S., & Hu, R. (2018). Graphene Oxide Dielectric Permittivity at GHz and Its Applications for Wireless Humidity Sensing, Science. Reports, 8:43.

[22] Gu, J., Lv, Z., Wu, Y., Guo, Y., Tian, L., Qiu, H., Li, W., & Zhang, Q. (2017) Dielectric thermally conductive boron nitride/polyimide composites with outstanding thermal stabilities via in-situ polymerization electrospinning-hot press method, Composites: Part, 94: 209-216.

[23] Huang, L., Liu, X., & Yu, R. (2018). Enhance Microwave Absorption Properties of Rod Shaped Fe_2O_3/Fe_3O_4/ MWCNTs composites, Prog. Nat. Sci.: Mater. Int'l, 28:288- 295.

[24] Qin, M., Zhang, L., & Wu, H. (2022). Dielectric Loss Mechanisms in Electromagnetic Waves Absorbing Materials, *Adv. Sci.*, 9, -VCH GmbH.

[25] Vikram, S. Y., Devendra, K. S., Yashpal S., & Dhubkarya, D.C. (2010). The Effect of Frequency and Temperature on Dielectric Properties of Pure Poly Vinylidene Fluoride (PVDF) Thin Films.

[26] Majdzadeh-Ardakani, K., Sadeghi, B., & Naderi, G. (2017). Investigation on rheological, mechanical and morphological properties of PVDF/BaTiO nanocomposites. Polymer Science, Series A, 59(4), 548-556.

[27] Seong, H. K., Lee, S. Y., Zhang, Y., Park, S. J., & Gu, J. (2023). Carbon-Based Radar Absorbing Materials toward Stealth Technologies. Advanced Science.

[28] Rahman, H. (2013). Fundamental Principles of Radar, CRC Press Taylor & Francis.